Effects of Flexible Splitter Plate in the Wake of a Cylindrical Body

S. Teksin and S. Yayla[†]

Deparment of Mechanical Engineering, Yuzuncu Yil University,Van, 65080, Turkey

†*Corresponding Author Email: syayla@yyu.edu.tr*

ABSTRACT

In the wake of the bluff bodies rigid splitter plates are known to control vortex shedding. In this study, the problem of flexible splitter plate in the wake of circular cylinder was investigated using Particle Image Velocimetry (PIV) experimentally. In this case; the splitter plate which has a certain amount of modulus of elasticity freely deforms along its length because of the fluid forces on plate. The diameter of cylinder, D was 60 mm while the Reynolds number based on the cylinder diameter is kept constant as 2500, the characteristics length of the control element, L was tested for four different cases that the values of L/D were 0, 1.25, 2.25, 2.5 in the investigation. As a consequence, turbulent kinetic energy, TKE, velocity vector field $<V>$, vortex$<\omega>$, Reynolds stress $<u'v'>$, root mean square of streamwise and transverse velocities, $<u_{rms}>/U$, $<v_{rms}>/U$ were analyzed. It is found that the variable parameter of L/D affects the flow structures and also noted that it decreased maximum level of all characteristic values.

Keywords: Cylinder; Particle image Velocimetry; Passive control; Vortex shedding; Flexible splitter plate.

NOMENCLEATURE

D	diameter of the circular cylinder	$u'u'$	streamwise Reynolds normal stress
h_L	height of the laser sheet	$u'v'$	Reynolds shear stress
h_w	water level	V	velocity vector
L	length of control element	V_{rms}	intensity of turbulence in transverse direction
L/D	aspect ratio	$v'v'$	transverse Reynolds normal stress
Re_D	Reynolds number		
TKE	normalized turbulent kinetic energy	ω	vorticity
U	free stream velocity)	$<>$	time-average value of quantity
U_{rms}	intensity of turbulence in streamwise direction		

1. INTRODUCTION

Some researchers who especially deal with fluid mechanics investigate about flow structure over a bluff body in the wake region downstream of the body. Some explanatory examples can be taken into consideration such as flow around an automobile, aircraft, space shuttle, bridge, building, chimney, cooling tower even electronical parts. A circular cylinder is widely used to investigate the structures and it is chosen because of its geometrical simplicity. In such engineering application, noises and vibrations which can be occurred due to the interactions between wakes, shear layers, vortices and Kármán vortex streets are quite important as mentioned by Sumner *et al.* (2004). Actually,

approach of controlling the vortex can be classified into two main categories. Controlling the flow structures of any body is provided by active system such as acoustic or any other energy input. For instance, heating the cylinder, Lecordier *et al.* (1991), rotary oscillation of the cylinder at a suitable frequency Lee and Lee (2008), Naim *et al.* (2007), acoustics excitations Blevins (1985), and control of the electromagnetic force. Kim and Lee (2001) can be noticed as the example of active application studies. Tabatabaeian *et al.* (2015) examined effects of various configurations of plasma actuator on the flow characteristics around the cylinder. They showed decrease in pressure coefficient of the used geometry. In another investigation, Sohankar *et al.* (2015) demonstrated

square cylinder arrangement to show the effect of uniform suction and blowing on the wake region and heat transfer of numerical experiment with Re=70-150. They reported that the lift and drag fluctuations were weakened and the maximum reduction on the drag force are between %61 and %72 for optimum Reynolds range, Re=70-100 and 150.

Although there are two main control methods called passive and active, most of the investigators have chosen the passive manner which is easy to examine the structures of the wake region. Therefore, control of flow around a body especially circular cylinder was investigated in shallow and deep water by lots of scientists or engineers Wolanski *et al.* (1984), Chen and Jirka (1995), Akilli *et al.* (2004, 2005, 2008).

A number of investigators Roshko (1954), Bearman (1965) have studied the rigid splitter plates in the wake on any shape of submerged body. They showed that splitter plates which have a certain length control the vortex shedding instabilities in wake flow region. Set-up of Assi *et al.* (2009) and Gu *et al.* (2012) used a hinged rigid splitter plate rear of the cylinder. These investigations showed that the plate oscillates; reach on equilibrium position or at an angle to the free stream flow direction. Apelt *et al.* (1973) and Apelt and West (1975) examined the effects of attaching a wake splitter plate behind a circular cylinder. In their investigation, they continuously changed the length of the splitter plate. They reported that they could determine frequencies in the wake region even for long splitter plates (L/D>5). For the splitter plate longer than 2D, drag reduced till to 5D splitter plate length. It is obvious from the results of near the wake region, effect of rigid splitter plate can be varied by altering the length.

These papers explain that flow characteristics can be passively controlled by changing shape of the body or attaching external devices to the target body which is tested. Akilli *et al.* (2005) constructed the experimental setup attaching the splitter plate which has a distance between plate and the cylinder. The length of splitter plate was equal to the cylinder diameter, D. It was noticed that the splitter plate significantly suppressed the vortex shedding for the gap, which was the distance between base of the cylinder and leading edge of the plate, changed from 0 to 1.75D. Xu *et al.* (2010) passively controlled the flow past a wavy cylinder, nearly 26% reduction of the drag coefficient of the wavy cylinder was much smaller than that of the circular cylinder. Also, fluctuation velocities suppressed to approximately zero. Pinar *et al.* (2015) performed experimental investigation to get information on the flow characteristics around perforated cylinders using Particle Image Velocimetry technique. They declared that the porosity sufficiently effects on the control of vortex structures where shear layers were elongated. On the other hand, for some set ups, just opposite situation is truly needed. Yayla (2015) constructed a remarkable plate heat exchanger with slotted cylinders located staggered configuration. By

grooving a slot onto each cylinder, he realized that turbulences are increased with respect to bare cylinder case. Pasiok *et al.* (2010) analyzed the mechanisms of transportation of bed material grains from the scour hole numerically. They reported that simulations verify strong interdependence of horseshoe vortex and wake vertical vortices system. It is proposed that all the main flow structures around a pier must be considered as a one system rather. Kuhl *et al.* (2012) constructed flexible cantilevered body attached to in a two dimensional circular cylinder by using numerical simulation. They showed that periodic vibration in sub-critical flow status. Also they demostrated that increase in Reynolds number, reduction in frequency of vortex shedding.

In this present work, control of the vertical circular cylinder attached with fully flexible sheet as a splitter plate in the wake flow region was experimentally investigated using particle image velocimetry (PIV) technique. The vortex formation around the vertical bluff body was passively controlled and under constant deep water flow regime, in order to investigate some flow structures are studied such as Velocity vectors, Turbulent Kinetic Energy, Reynolds Stress values, vortex and other flow characteristics. It is intended that minimizing the destruction some whole or part a body by suppressing the vortex shedding.

2. EXPERIMENTAL SETUP AND INSTRUMENTATION

The present experiment was conducted in a 8000 x 1000 x 750 mm^3 closed loop water channel in the Mechanical Engineering Department Fluid Mechanics Laboratory at Cukurova University. A pump was used to circulate the water driven by the electric motor had changeable speed. It provides us the mean flow in the test section which has 15 mm thick Plexiglas material. The water of deep level *(h$_w$)* is 600 mm. Schematic representation of the setup such as top view of the test section, all dimensions, laser sheet location were shown in Fig. 1. All experiments were carried out above the platform having a length of 2300 mm. The distance between leading edge of the platform and the cylinder position was 2000 mm. Diameter of used cylinder was 60 mm and free stream flow velocity was 41 mm/s, resulting in a Reynolds number, Re$_D$=2500 based on the cylinder diameter. Splitter plates have four different length (L=0 mm, 75 mm, 135 mm, 150 mm). The splitter plates have 1400 N/mm^2 modulus of elasticity and the thickness of the splitter plate is 80 micron. Circular cylinder is made of transparent Plexiglas material for accessibility of PIV measurements. In all of the experiment demonstrated here, the investigation of the flow structures around a vertical circular cylinder was implemented by altering the length of the splitter plate. Free stream of water velocity was kept constant and all the experiments were installed in fully developed flow condition.

The experiments were performed with Dantec

Dynamics PIV system and its installed Flow manager software on a computer. The target area was illuminated by laser sheet approximately 1 mm height using a pair of double pulsed Nd: YAG (yttrium aluminum garnet) laser units. Energy output of the laser equipment is 120 mJ and 532 nm wavelength. The laser sheet was located to 5 mm below the top level of the cylinder. Image was performed by a CCD (Charged Coupled Display) camera having resolution of 1024 X 1024 pixels with a Nikon 60 mm lens. A total of 7227 (99x73) velocity vectors were achieved for an instantaneous velocity field with frequency of 15 Hz. The magnification factor *M* was set 21.47 from the image positioned on the laser sheet in flow region. 350 total images were captured and recorded to obtain averaged velocity vectors and other structural properties of the flow region. Silver coated metallic small particles with 12 µm diameter were seeded to water with the density of 1100 kg/m^3. Using local median filter technique spurious bad velocity vectors were removed for smooth and well defined results.
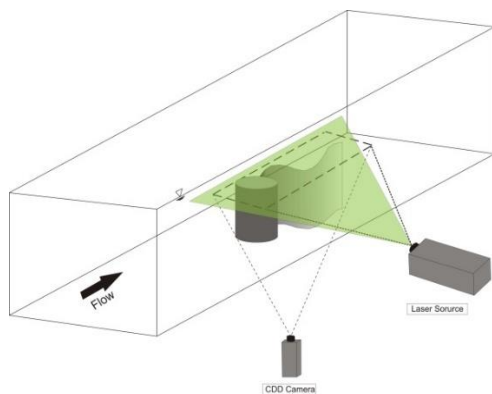

Fig. 1. Schematic of the experimental system of setup basically.
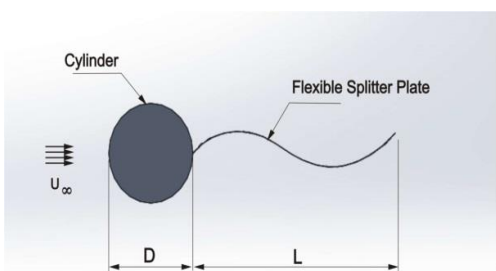
Fig. 2. Representation of the setup parameters detailed.

The raw velocity vector field was determined from this displacement vector field using the time interval between pulses. Less than %5 spurious velocity vectors were removed using the local median filter technique and replaced by using a bilinear least square fit technique surrounding to forestall changes in the velocity vector field using

Gaussian smoothing method. The vorticity level at each grid was calculated from the flow around the eight neighboring points. The factors contributing to uncertainty in the velocity measurement using the PIV method were critically assessed by Westerweel (1994) who concluded that uncertainty estimation in the velocity measurement was less than 2%. A non-post interrogation method of reducing errors and clearing spurious velocity vectors from particle image velocimetry (PIV) was applied by Hart (2006). Unlike methods that rely on the accuracy or similarity of neighboring vectors, errors are eliminated before correlation information is discarded using available spatial and/or temporal data. Gallanzi (1998) demonstrated broad information about the uncertainty affect by PIV arrangement.
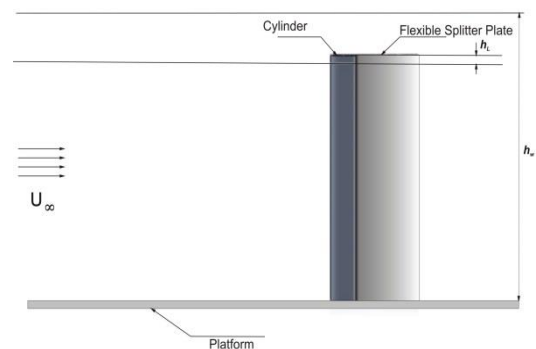
Fig. 3. Definition of the parameters.

3. RESULTS AND DISCUSSION

The flow structures of time averaged velocity vectors *(<V>)*, vorticity *(<ω>)* and Reynolds stress *($<u'v'>/U^2$)* at the height of the 5 mm below the top level of the cylinder were illustrated in Fig. 4. In order to examine the effect of the flexible splitter plate, additional material was attached to rear of the circular cylinder at different dimensionless length ranging from L/D=1.25 to L/D=2.5. Reynolds number of *(Re_D)* based on the cylinder diameter was 2500. PIV experiments show that the plate length have a considerable effect on the flow characteristics. Time averaged flow characteristics shown in Fig. 4 have an almost symmetrical pattern with respect to centerline of the wake flow region for different dimensionless lengths of the plate. The vorticity has been well described in supported corresponding Reynolds stress images. Low velocity region which is called the wake region substantially elongates along the streamwise direction with increasing length of the flexible splitter plate as shown velocity vector maps in the first column of Fig. 4. While wake flow region for L/D=1.25 was narrowed with respect to other configuration, this zone in wake also extends to downstream direction. The second column of the Fig. 4 compares the vorticity contours having the four different lengths against to bare case. Here, while the solid lines represent positive (counter clockwise), dashed lines show negative (clockwise)
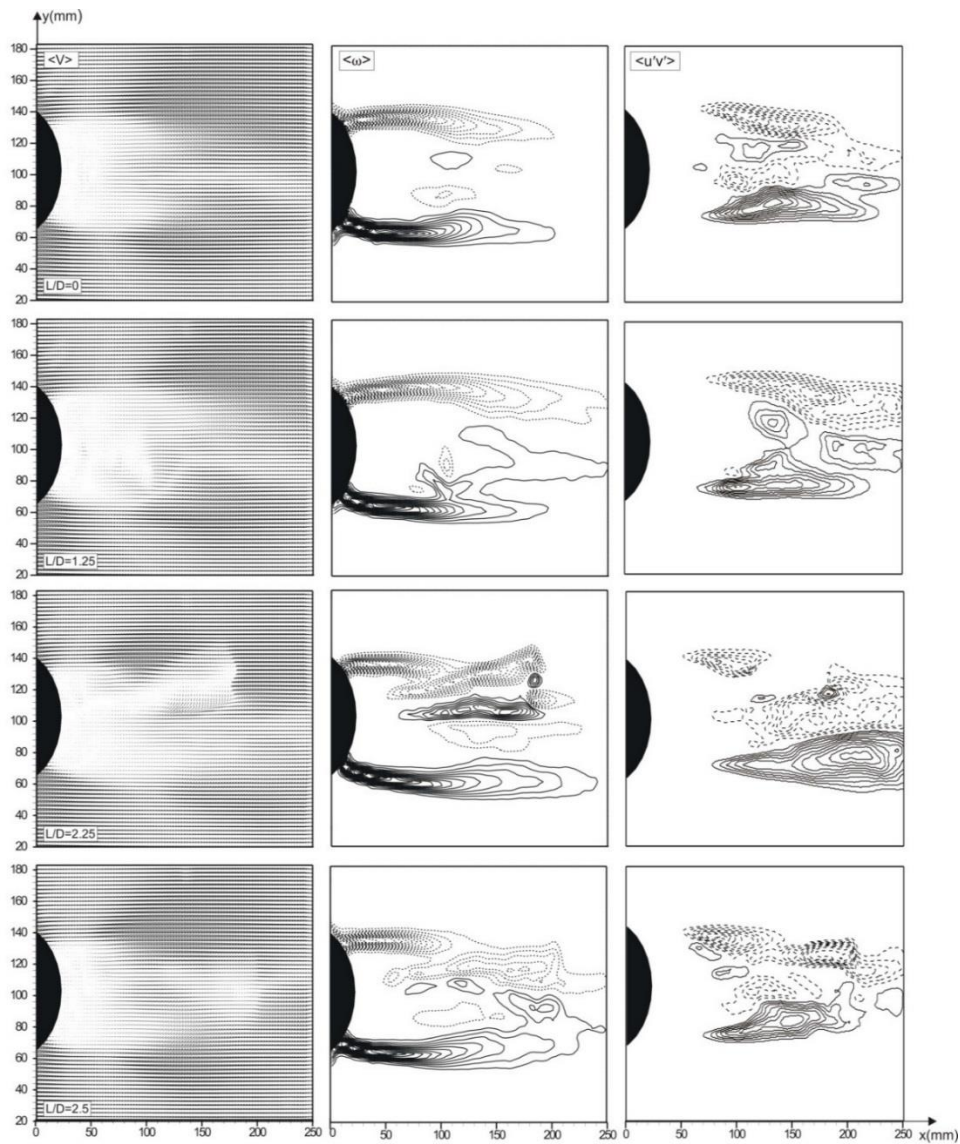
**Fig. 4. Velocity vector field, vorticity contours and Reynolds Stress.**

vorticity layers. Minimum and incremental values are $[<\omega>]_{min}=\pm0.5$ s^{-1} and $\Delta[<\omega>]=0.5$ s^{-1} for vorticity respectively. When the flexible splitter plates were added to the rear of the circular cylinder, the plates formed a secondary vorticity contours in the wake flow region both at L/D=2.25 and 2.5. However, maximum level of these contours values stay nearly same $[<\omega>]_{max}$ ±7.4 - 7.5.

In the third column of Fig. 4 Reynolds stress $<u'v'>/U^2$ contours which have both negative and positive contours images for all cases were shown. This figure remarked that high concentrations of the stresses were shifted to the x direction with respect to bare cylinder. The low values of Reynolds stress correlation zone placed in the location of both side of the cylindrical body. As the fluid flows downstream value of the Reynolds stress increases and reaches the peak point nearly at the center of the contours. Minimum and incremental values of Reynolds

stress contours are $[<u'v'>/U^2]_{min}=\pm0.01$ and $\Delta[<u'v'>/U^2]=0.005$ respectively. While in case of bare cylinder status, maximum value of Reynolds stress was 0.05. The peak value of Reynolds stress decreases to 0.032 for L/D=1.25. It means that the presence of a very short flexible splitter plate is effective in decreasing the maximum level of Reynolds stress. When the length of the flexible splitter plate was extended, this value continues to decrease and drops until level of 0.028 for L/D=2.5. It can be said that the significant decrease in the Reynolds stress correlation is closely related to reduction in the drag force of circular cylinder (Fujisawa *et al.* 2003; Kim *et al.* 2006). While the peak value of concentration of Reynolds stress obtained for L/D=2.5 case is 0.055 the peak value took place is 0.045 for bare cylinder case.

Patterns of root mean square of streamwise fluctuations which are defined as turbulent flow characteristics $<u_{rms}>/U$ flexible strip attached body

compared with bare cylinder case are shown in Fig. 5. Minimum and incremental values are $[<u_{rms}>/U]_{min}=0.02$, $\Delta[<u_{rms}>/U]=0.02$ respectively. The turbulence level in the wake of the circular cylinder is increased by formation of fluctuations. In other words, turbulence intensities $<u_{rms}>/U$ and $<v_{rms}>/U$ increase through the streamwise direction. Very symmetrical contours can be seen for bare cylinder and indicates the maximum level of $<u_{rms}>/U$ value 0.44. These rms of velocity components gradually decreases until L/D=2.25 about 0.3 level, stay constant for longer ratios. The location of the maximum value of $<u_{rms}>/U$ is kept constant in the same distance from the cylinder surface. Contours of $<u_{rms}>/U$ are clustered far downstream of the cylinder at both sides and seperated from cylinder as seen in second column of Fig. 5. Images L/D=0 to L/D=2.5 for $<v_{rms}>/U$ are presented in Fig. 6 and minimum and incremental values are $[<v_{rms}>/U]_{min}=0.02$, $\Delta[<v_{rms}>/U]=0.02$. Transverse fluctuation velocity $<v_{rms}>/U$ were in contact to the circular cylinder. Peak value of transverse velocity fluctuations for bare cylinder case is 0.3. Moreover, at the range from L/D=1.25 to 2.5, the peak values decreased significantly and reached to level of 0.19 for L/D=2.5 as a result of momentum transfer to the flexible splitter plate and absorbed of the energy by the attached body.
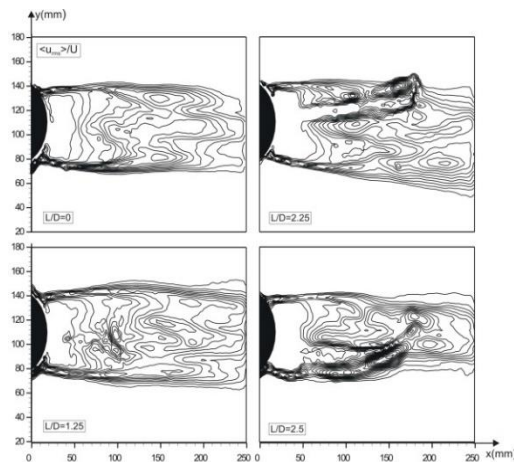
**Fig. 5. Root mean square of streamwise velocity fluctuations u_{rms}/U.**

The variation of peak values of normalized streamwise Reynolds stress $<u'u'>$ and transverse Reynold stress $<v'v'>$ based on the flexible plate length ratio (L/D) are given in Figs. 7, 8 to introduce their effects on the impairment of turbulent kinetic energy, (TKE). These Reynolds stress values are non dimensionalization by being divided them with square of free stream velocity. In respect of thought of Feng and Wang (2010) and Schafer *et al.* (2009), turbulence mixing can form an estimate of TKE, helps us to comprehend the dynamics of vortices. While the minimum and incremental values of the contours for streamwise Reynolds normal stress are $[<u'u'>]_{min}=0.01$ and $\Delta[<u'u'>]=0.005$ respectively, for transverse Reynolds normal stress are $[<v'v'>]_{min}=0.01$ and $\Delta[<v'v'>]=0.002$ respectively.

The peak value of both Reynolds normal stresses reduces with increasing the flexible splitter plate length. However, the rate of decrease in transverse Reynolds normal stress is much more than streamwise Reynolds stress as it can be seen Fig. 8. The maximum values of normalized streamwise and transverse Reynolds normal stresses are 0.19 and 0.09 for bare cylinder case respectively. These values decreases to 0.145 and 0.042 for L/D=1.25 and 0.13 and 0.036 for L/D=2.5. On the other hand, because of the fact that changes in the peak value of Reynolds stresses are negligible level for more than L/D=2.5, the other lengths of flexible splitter plates were not added to this paper. As could be seen from the data, these numerical values present that transverse Reynolds normal stresses have significant effect on the attenuation of TKE with respect to the effect of streamwise Reynolds normal stress.
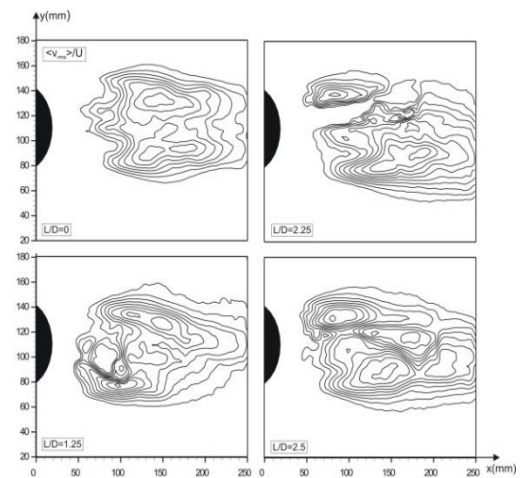


Fig. 6. Transverse velocity fluctuations v_{rms}/U.

Figure 9 presents variations of the contours of normalized (TKE) as a function different plate length of L/D for all graphs. Minimum and incremental value of turbulent kinetic energy are $[<TKE>]_{min}=0.005$ and $\Delta[<TKE>]=0.01$ respectively. TKE increases initially along the downstream direction starting from near of the circular cylinder and rises its maximum value at a point close the distance of 1.5D for L/D=1.25 and 2.5D for L/D=2.25 and 2.5 position along the centerline location in wake region respectively. It means that at the trailing edge of the flexible splitter plate, maximum TKE level is formed. Then, it decreases progressively along the downstream direction. Compared to the plate attached cylinder case, contours of the TKE lines which are located in both sides of the cylinder are symmetrical as Reynolds Stress $(<u'v'/U^2>)$, rms of the streamwise velocity fluctuations $<u_{rms}>/U$. On the other hand, due to the fact that the formation of large scale vortices is suppressed by the flexible splitter plate, the entrainment of the freestream flow into the wake region forestall and the peak value of TKE does not happen along the symmetry line anymore. There are no negligibly changes for size of wake region and the peak value of TKE for all cases compared to bare cylinder case.
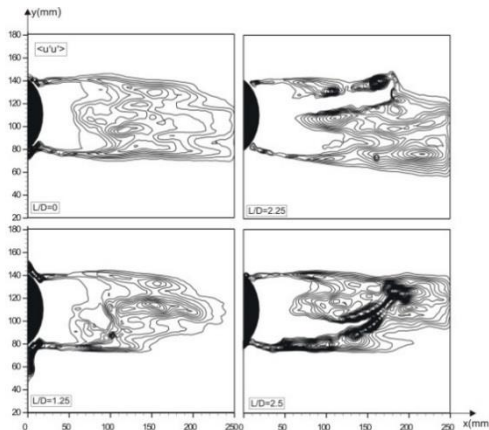
Fig. 7. Normalized streamwise Reynolds stress and transverse normal stress.
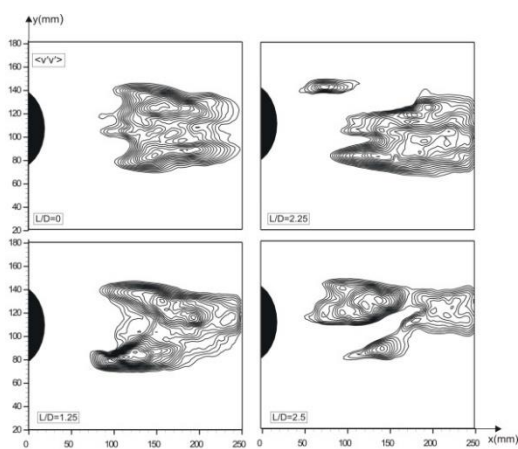
Fig. 8. Distribution of normalized and transverse normal stress.
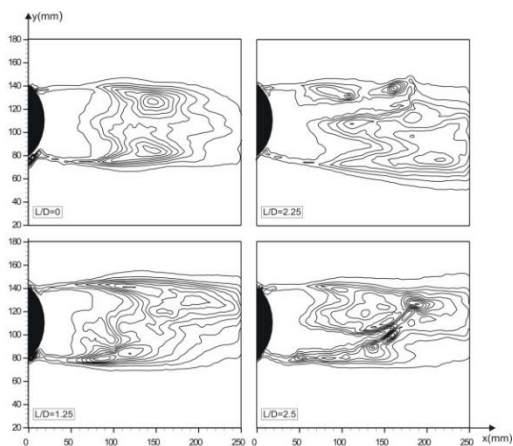
Fig. 9. Turbulent Kinetic Energy (TKE).

When the maximum value of TKE for the bare cylinder case is approximately 0.19, the peak value of TKE for the smallest flexible splitter length, L/D=1.25, reduces to approximately 0.145. Even, this decrease is more evident for the ration of L/D=2.25 which nearly %38 means 0.09. The reduction in the peak value of TKE means that the existence of the flexible splitter plate located downstream of the circular cylinder strongly suppresses the large scale vortices that transport

fresh fluid into the wake region. Both the streamwise Reynolds normal stress and transverse Reynolds normal stress have same influence on the weakening of turbulent kinetic energy such as approximately %51 - 52. However, the variation of TKE of L/D more than 2.25 presents a small difference compared to other ratios.

4. CONCLUSION

The flow structure in the wake region of circular cylinder with attached flexible splitter plate which was located in rectangular water channel have been examined experimentally in deep water using the Particle Image Velocimetry (PIV) Technique. The results were taken at a distance of 5 mm below the top height of the cylinder by illuminating with laser sheet. The effects of the flexible splitter plate length, ranging from 75mm (L/D=1.25) to 150 mm (L/D=2.5), on the suppression of vortex shedding were defined by the time averaged velocity vector correlation, related vorticity field and turbulent statistics such as streamwise and transverse Reynolds normal stress, root mean square of streamwise and transverse velocities, turbulent kinetic energy (TKE), Reynolds shear stress and vortex shedding. Turbulent flow characteristics of wake zone behind the cylinder altered immediately with even the existence of the smallest flexible splitter plate. Increasing the splitter plate length results in a decrease of peak value of the any kind of structures until the L/D=2.5. After this flexible splitter plate length, major changes cannot be obtained. In other words, while almost all of longer ratios remain approximately constant, significant amendments in turbulent statistics are acquired till to L/D=2.5 and for longer length values, inconsiderable changes occur in flow characteristics of the cylinder wake zone and because of the fact that the flow is unsteady, alterations of flow characteristics are nearly similar for most of the instantaneous views. Namely, since the amount of momentum which causes to deformation of structure such as bridges, pipelines or marine constructions transferred through the flexible splitter plate, reductions in the turbulences were formed.

ACKNOWLEDGMENT

The authors very much indebted to Professor B. Sahin for letting them carry out this experimental study at the Fluid Mechanics Laboratory of Cukurova University, TURKEY.

REFERENCES

Akilli, H., A. Akar and C. Karakus (2004). Flow characteristics of circular cylinders arranged side-by-side in shallow water. *Flow Meas. Instrum* 15(4), 187–197.

Akilli, H., B. Sahin and N. F. Tumen (2005). Suppression of vortex shedding of circular cylinder in shallow water by a splitter plate.

Flow Meas. Instrum 16, 211–219.

Akilli, H., C. Karakus, A. Akar, B. Sahin and N. F. Tumen (2008). Control of vortex shedding of circular cylinder in shallow water flow using anattached splitter plate. *J. Fluids Eng. Trans. ASME* 130, 1–11.

Apelt, C. J., G. S. West and A. A. Szewczyk (1973). The effects of wake splitter plates on bluff–body flow in the range 104 < R < 5 × 104. *J. of Fluid Mech*. 61(1), 187–198.

Apelt, C. J., G. S. West and A. A. Szewczyk. (1975). The effects of wake splitter plates on bluff–body flow in the range 104 < R < 5 × 104 Part 2. *J. of Fluid Mech.* 71(1), 145–160.

Assi, G., P. W. Bearman and N. Kitney (2009). Low drag solutions for suppressing VIV of circular cylinders. *J. of Fluids and Struct.* 25, 666–675.

Bearman, P. W. (1965). Investigation of flow behind a two dimensional model with a blunt trailing edge and fitted with splitter plates. *J. of Fluid Mech.* 21, 241–255.

Blevins, R. D. (1985). The effect of sound on vortex shedding from cylinders. *J. of Fluid Mech.* 161, 217–237.

Chen, D. and H. Jirka (1995). Experimental study of plane turbulent wakes in a shallow water layer. *Fluid Dyn. Res.* 16 11–41.

Cu, C. Y., L. W. Chen and X. Y. Lu (2010). Large-eddy simulation of the compressible flow past a wavy cylinder. *J. of Fluid Mech.* 665, 238–273.

Feng, L. H. and J. J. Wang (2010). Circular cylinder vortex-synchronization control with a synthetic jet positioned at the rear stagnation point. *J. Fluid Mech.* 662, 232-259.

Fujisawa, N. and G. Takeda (2003). Flow control around a circular cylinder by internal acoustic excitation. *J. Fluids Struct.* 17, 903-913.

Gallanzi, M. F. (1998). High aacuracy measurement of unsteady flow using digital particle image velocimetry. *Optic & Laser Tech.* 30(6-7), 349-359.

Gu, F., J. S. Wang, X. Q. Qiao X and Z. Huang (2012). Pressure distribution, fluctuating forces and vortex shedding behavior of a circular cylinder with rotatable splitter plates. *J. of Fluids and Struct.* 28, 263–278.

Hart, D. P. (2006). PIV error correction. *Exp. in Fluids* 40, 13-22.

Kim, S. J. and C. M. Lee (2001). Control of flows around a circular cylinder: suppression of oscillatory lift force. *Fluid Dyn. Res.* 29, 47–63.

Kim, W., J. Y. Yoo and J. Sung (2006). Dynamics of vortex lock-on in a perturbed cylinder wake. *Phys. Fluids* 18, 074103.

Kuhl, J. M. and P. E. Des Jardin (2012). Power production locality of bluff body flutter mills using fully coupled 2-D direct numerical simulation. *Journal of Fluids and Structures* 28, 456-472.

Lecordier, J. C., L. Hamma and P. Parantheon (1991). The control vortex shedding behind heated cylinders at low Reynolds numbers. *Exp. in Fluids* 10, 224–229.

Lee, S. J. and J. Y. Lee (2008). PIV measurements of the wake behind a rotationally oscillating circular cylinder. *J. of Fluids and Struct.* 24, 2–17.

Naim, A, D. Greenblatt, A. Seifert and I. Wygnanski (2007). Active control of a circular cylinder flow at transitional Reynolds numbers. *Flow, Turbulence and Combustion* 78, 383–407.

Pasiok, R. and Stilger-Szydło, E. (2010). Sediment particles and turbulent flow simulation around bridge piers. *Archives of Civil and Mech Eng*, X (2), 67-79.

Pinar, E., G. M. Ozkan, T. Durhasan, M. M Aksoy, H. Akilli and B. Sahin (2015). Flow structure around perforated cylinders in shallow water. *J. of Fluid Mech.* 55, 52-63.

Roshko, A. (1954). On the drag and shedding frequency of two dimensional bluff bodies. *NACA Technical Notes* 3169.

Schafer, F., M. Breuer and F. Durst (2009). The dynamics of the transitional flow over a backward facing step. *J. Fluid Mech.* 623, 85-119.

Sohankar A., M. Khodadadi and E. Rangraz (2015). Control of fluid flow and heat transfer around a square cylinder by uniform suction and blowing at low Reynolds numbers. *Computers and Fluids* 109, 155–167.

Sumner, D., J. L. Heseltine and O. J. P. Dansereau (2004). Wake structure of a finite circular cylinder of small aspect ratio. *Exp. in Fluids* 37, 720–730.

Tabatabaeian S., M. Mirzaei, A. Sadighzadeh, V. Damideh and A. Shadaram (2015). Experimental Study of the Flow Field around a Circular Cylinder Using Plasma Actuators. *J. Applied Fluid Mechanics* 8(2), 291-299.

Waterwheel, J. (1994). Efficient detection of spurious vectors in particle image velocimetry data sets. *Exp. in Fluids* 16, 236-247.

Wolanski, E., I. Imberger and M. L. Heron (1984). Island wakes in shallow coastal waters. *J. Geophys. Res.* 89(C6), 10553–10569.

Yayla, S. (2015). Flow Characteristic of Staggered Multiple Slotted-Tubes in the Passage of Fin Tube Heat Exchanger. *Strojniški vestnik J. of Mech. Eng.* 59(7-8), 462-472.